FEBS Letters

FEBS PRESS science publishing by scientists

COMMUNICATION

Hsp90 and metal-binding J-protein family chaperones are not critically involved in cellular iron–sulfur protein assembly and iron regulation in yeast

Felipe A. Carvalho[1,2,3], Ulrich Mühlenhoff[2,3], Joseph J. Braymer[2,3], Vasilij Root[2,3], Martin Stümpfig[2,3], Carla C. Oliveira[1] and Roland Lill[2,3]

1 Department of Biochemistry, Institute of Chemistry, University of Sao Paulo, Brazil
2 Institut für Zytobiologie, Philipps-Universität Marburg, Germany
3 Zentrum für Synthetische Mikrobiologie Synmikro, Marburg, Germany

Correspondence
C. C. Oliveira, Department of Biochemistry, Institute of Chemistry, University of Sao Paulo, Av. Prof. Lineu Prestes 748, Sao Paulo, SP 05508-000, Brazil
Tel: +55 11 3091 9197
E-mail: ccoliv@iq.usp.br
R. Lill, Institut für Zytobiologie, Philipps-Universität Marburg, Karl-von-Frisch-Str. 14, 35032, Marburg, Germany
Tel: +49 6421 286 6449
E-mail: lill@staff.uni-marburg.de

Felipe A. Carvalho and Ulrich Mühlenhoff contributed equally to this article

[Correction added on 20 June 2023, after first online publication: Peer review history statement has been added.]

(Received 27 January 2023, revised 7 March 2023, accepted 10 March 2023, available online 30 March 2023)

doi:10.1002/1873-3468.14612

Edited by Peter Brzezinski

Systematic studies have revealed interactions between components of the Hsp90 chaperone system and Fe/S protein biogenesis or iron regulation. In addition, two chloroplast-localized DnaJ-like proteins, DJA5 and DJA6, function as specific iron donors in plastidial Fe/S protein biogenesis. Here, we used *Saccharomyces cerevisiae* to study the impact of both the Hsp90 chaperone and the yeast DJA5-DJA6 homologs, the essential cytosolic Ydj1, and the mitochondrial Mdj1, on cellular iron-related processes. Despite severe phenotypes induced upon depletion of these crucial proteins, there was no critical *in vivo* impact on Fe/S protein biogenesis or iron regulation. Importantly, unlike the plant DJA5-DJA6 iron chaperones, Ydj1 and Mdj1 did not bind iron *in vivo*, suggesting that these proteins use zinc for function under normal physiological conditions.

Keywords: heat shock proteins; iron chaperones; iron–sulfur cluster; mitochondria; protein folding

Iron–sulfur (Fe/S) proteins involved in numerous central biological functions such as photosynthesis and respiration, metabolic processes, protein translation, DNA synthesis and repair, and sensing of environmental conditions [1]. The biogenesis of Fe/S proteins in all kingdoms of life is catalyzed by evolutionarily conserved multi-protein assembly systems that require sources of iron and sulfur for the *de novo* synthesis, trafficking, and apoprotein insertion of Fe/S clusters [2–8]. In eukaryotes, Fe/S protein formation is initiated in mitochondria by the iron–sulfur cluster assembly (ISC) machinery, which comprises up to 18 known proteins, most of which are also present in bacteria (Fig. S1) [2,4]. Biosynthesis of cytosolic and nuclear Fe/S proteins additionally requires the mitochondrial ABC transporter Atm1 and the cytosolic iron–sulfur protein assembly (CIA)

Abbreviations
AP-MS, affinity purification and mass spectrometry; CIA, cytosolic iron–sulfur protein assembly; Fe/S, iron–sulfur; ISC, iron–sulfur cluster assembly; SGA, synthetic genetic array; SUF, sulfur mobilization; Y2H, yeast two-hybrid; ZFLR, zinc-finger-like region.

system (Fig. S1) [3,9]. Plants further harbor the bacteria-derived sulfur mobilization (SUF) system for the maturation of Fe/S proteins in plastids [7,10]. Many of the ISC and CIA components are essential for cell viability, underscoring the importance of Fe/S proteins and their biogenesis in the eukaryotic cell [4,11–13].

In addition to the synthesis, trafficking, and insertion of Fe/S clusters, the receiving apoproteins need to be folded properly to be competent for cluster integration, yet little is known about this process. Further, the apoproteins need to escape preinsertion degradation, since many target apoproteins are unstable and undergo proteolysis, when Fe/S clusters are not inserted. This is reflected by low *in vivo* Fe/S protein levels in cells with Fe/S cluster assembly defects [14–16]. Therefore, it seems likely that the Fe/S apoproteins are clients of the cellular folding machineries. Yet, so far only one chaperone system has been identified with importance for Fe/S protein assembly, the DnaK-DnaJ-like (or Hsp70-Hsp40-like) chaperones in mitochondria [17–19]. However, the *S. cerevisiae* mitochondrial Hsp70 Ssq1 and its DnaJ-type co-chaperone Jac1 are not involved in apoprotein folding as general folding helpers. Rather, these proteins loosen the [2Fe-2S] cluster after its synthesis on the scaffold protein Isu1 for specific transfer to the mitochondrial monothiol glutaredoxin Grx5 (Fig. S1) [17,18,20,21]. Thus, this chaperone system is dedicated to the mitochondrial ISC protein Isu1 as its sole client. While the yeast Ssq1-Jac1 proteins function similarly to HscA-HscB of the bacterial ISC system [8,21], most eukaryotes make use of the canonical mitochondrial Hsp70 (e.g., human HSPA9) that is also generally used for protein folding and import [17–19]. In these cases, only the Jac1 co-chaperone fulfills a dedicated function with Isu1 as its specific client. The human Jac1 homolog HSC20 has been further suggested to facilitate Fe/S cluster transfer not only to glutaredoxin 5 (GLRX5) but directly to some Fe/S target apoproteins *via* specific protein–protein interaction [22,23]. An additional apoprotein folding function of HSC20 has not been investigated so far. Finally, the mitochondrial Hsp60 chaperonin (homolog of bacterial GroEL) specifically facilitates the maturation of aconitase by promoting its folding [24,25]. However, closer analysis of the possible role of this and other general chaperone systems by *in vivo* studies is hampered by the pleiotropic phenotypes induced by the lack of these essential folding machines.

The cytosolic Hsp90 chaperone acts in late stages of protein maturation of a narrower range of clients that frequently become unstable upon Hsp90 inhibition [26–29]. Large-scale interactome analyses by combined affinity purification and mass spectrometry (AP-MS) identified the CIA or iron regulation proteins Nbp35, Grx3, Grx4, and Fra1 as Hsp90 interactors (Fig. S1, green stars) [30]. Further, in a high-throughput yeast two-hybrid (Y2H) screen, the CIA protein Cfd1 was found as an Hsp90 interactor [31]. A genetic interaction of Hsp90 with iron-regulatory proteins Aft2 and Bol2 (former name Fra2 [32]) was described in a synthetic genetic array (SGA) analysis [33]. Vice, versa, mapping of the CIA protein interactome by AP-MS identified Hsp90 as an interactor of Dre2 and Nbp35 (Fig. S1) [34]. Finally, a global study of the Hsp90-dependent proteome in yeast detected Aft1, the iron transporter Fet4, Isu2, Grx4, the ribonucleotide reductase subunit Rnr1, and the cytosolic Fe/S protein Leu1 as being downregulated in Hsp90-depleted cells [35]. As outlined below, we found the CIA factor Dre2 as a Pih1 (aka Nop17) interactor in a global Y2H screen. Pih1 is a member of the R2TP-complex, a dedicated Hsp90 co-chaperone involved in client discrimination and recruitment [33,36–38]. However, the putative mechanistic connection between Hsp90 and the suggested CIA and iron-regulatory clients has remained elusive. We therefore addressed the question of a specific functional role for Hsp90 in cellular Fe/S protein assembly and iron regulation using *S. cerevisiae* as a model.

Recently, two DnaJ family proteins, DJA5 and DJA6 from *Arabidopsis thaliana* were assigned as iron chaperones that deliver their bound iron to the $SUFBC_2D$ complex, the central Fe/S cluster synthesis complex of plastids [39]. Iron binding was shown both *in vivo* and *in vitro*, and occurs *via* a central zinc-finger-like region (ZFLR) that is absent in most other Hsp40 co-chaperones [7,10,40,41]. Loss of DJA5-DJA6 function affects plant viability, induces low levels of plastidial Fe/S proteins, impairs photosynthesis, and increases cellular iron levels [39]. To date, it is unknown whether DnaJ-like proteins similarly to DJA5-DJA6 function as iron chaperones in mitochondria or cytosol of eukaryotic cells, even though several J-proteins with a ZFLR have been identified in these compartments [41] (see below). In mitochondria, in contrast to plastids, the source of iron for *de novo* [2Fe-2S] cluster synthesis by the core ISC system is unknown, apart from the fact that iron is imported into the matrix by the solute carriers Mrs3 and Mrs4 (human mitoferrin 1 and 2; Fig. S1) [42–45]. In the cytosol, dedicated iron chaperones termed PCBP1 and PCBP2 (not present in fungi) insert their bound iron into various recipient proteins including the [2Fe-2S] cluster-containing GLRX3-BOLA2 complex [46–48]. Hitherto, a critical role for PCBP1-PCBP2 in general cytosolic Fe/S protein biogenesis has not been described. Here, we used *S. cerevisiae* as a model to address the question of whether

ZFLR-containing DnaJ-like proteins may function as putative iron donors for cellular Fe/S protein biogenesis.

Materials and methods

Yeast strains, cell growth, and plasmids

Saccharomyces cerevisiae strains (W303-1A, W303-1B or BY4742 background; Table S1) were grown in rich (YP) or Synthetic Complete minimal (SC) medium with the required supplements and the carbon sources 2% w/v glucose (YPD/SD), 2% w/v galactose (YPGal/SGal), or 3% w/v glycerol (YPGly) [49]. Strain Gal-HSC82/hsp82Δ was depleted by growth in SD medium for 30 or 40 h with one intermediate dilution into the fresh medium. Gal-YDJ1 was depleted by growth in SD medium for 24 h, or for 40 h with one dilution into fresh medium after 24 h. Gal-MDJ1, Gal-L-PIH1, and Gal1-HA-PIH1 cells were depleted for 40 h with one, or for 64 h with two dilutions into fresh medium. Plasmids used in this study are compiled in Table S2.

Yeast two-hybrid (Y2H) assay

The Gal4-based Y2H assay was performed according to the manufacturer's instructions (Takara Bio Inc., Shiga, Japan). The coding sequences of Pih1, the Pih1-interactor Tah1, and the CIA proteins were cloned into vectors pGBKT7-Gal4-BD (DNA-binding domain, bait) and pGADT7-Gal4-AD (activation domain, preys), respectively. pGBKT7 (Trp) and pGADT7 (Leu) constructs were transformed in Y2HGold and Y187 strains, respectively. After mating, diploid cells were selected in SD medium lacking Trp and Leu. Protein expression was evaluated by immunostaining using anti-GAL4-DNA-BD and anti-Gal4-AD antibodies (Takara Bio Inc.). Cell growth in the absence of His was used as a reporter for positive interactions. 2.5 mM 3-amino-1,2,4-triazole (3AT) was supplied to the medium to evaluate the interaction strength.

Biochemical assays

Detailed protocols for *in vivo* ^{55}Fe incorporation, enzymes, and *FET3*-promoter activities are published in dedicated methods papers [50–52]. Enzyme activities were measured in clarified whole-cell extracts obtained by glass-bead lysis. For (a) isopropyl malate isomerase (Leu1), isomerization of β-isopropyl malate was followed at 235 nm; (b) aconitase (Aco), reduction in $NADP^+$ was monitored at 340 nm in a coupled assay with isocitrate dehydrogenase (IDH); (c) malate dehydrogenase (MDH), NADH oxidation at 340 nm was recorded; (d) citrate synthase (CS), reaction of DTNB (5,5′-dithio-bis-2-nitrobenzoic acid) with the thiol group of coenzyme A was followed at 412 nm; (e) respiratory complex IV (cytochrome *c* oxidase, COX), oxidation of reduced cytochrome *c* was monitored at 550 nm. Enzyme activities for the tested strains were measured in parallel with corresponding wild-type control strains and normalized to MDH activity ($U \cdot mg^{-1}$). For sulfite reductase (SiR) activity, a plate-based assay was employed [34,53]. In brief, yeast cells were spotted on standard or Bi^{3+}-containing (0.1% w/v ammonium bismuth citrate, 0.3% w/v Na_2SO_3, and 1% w/v β-Ala) SD or SGal medium agar plates, and were incubated at 30 °C for 3 days. Cells were grown in liquid SGal medium overnight or SD medium for 10 h (for Gal-c82p82Δ) or 18 h (for Gal-PIH1 strains) prior to plating. Sulfide produced by holo-SiR yields a brown bismuth sulfide-containing precipitate in growing colonies.

FET3 promoter activity was measured based on the GFP fluorescence emission of whole yeast cells transformed with *pFET3*-GFP reporter plasmids [50]. Growth media were supplemented with 50 μM ferric ammonium citrate or 50 μM bathophenanthroline. For *in vivo* ^{55}Fe radiolabeling, yeast cells were grown for at least 16 h in an iron-poor medium and radiolabeled with $^{55}FeCl_3$ (Perkin-Elmer) for 2 h [50,52]. After glass-beads lysis clarified whole-cell extracts were used for immunoprecipitation of target proteins. The ^{55}Fe associated with the beads was measured by scintillation counting. Antibodies were raised in rabbits against recombinant purified proteins [54], except for antibodies against c-Myc and Pgk1, which were obtained from Santa Cruz Biotechnology Inc. (Santa Cruz, CA, USA) and Abcam (Cambridge, UK), respectively. Data analyses were carried out using PRISM 3 (GraphPad Software, San Diego, CA, USA). Immunostaining quantifications were carried out using IMAGE STUDIO LITE Software Version 5.2 from LICOR Biosciences (Lincoln, NE, USA).

Results and discussion

The Hsp90 co-chaperone Pih1 interacts with the CIA protein Dre2 in Y2H screens

While studying the interaction network of the Hsp90 co-chaperone Pih1, a component of the conserved R2TP (Rvb1-Rvb2-Tah1-Pih1) complex, we performed a genome-wide Y2H screen using Pih1 fused to the LexA-DNA-binding domain as a bait. Among other proteins, the global screen identified the CIA factor Dre2 as a positive hit. We therefore investigated the interaction between Pih1 and Dre2, as well as other members of the CIA machinery in a dedicated Gal4-Y2H approach (Fig. 1A, top). Tah1, another R2TP subunit known to tightly bind Pih1, was used as a positive control [33,36–38]. Expression of the CIA fusion proteins was verified by immunoblotting (Fig. 1B), and the Y2H system was validated using the manufacturer's controls (Fig. 1A, bottom). Activation of the reporter gene *HIS3*, leading to histidine-prototrophic recovery,

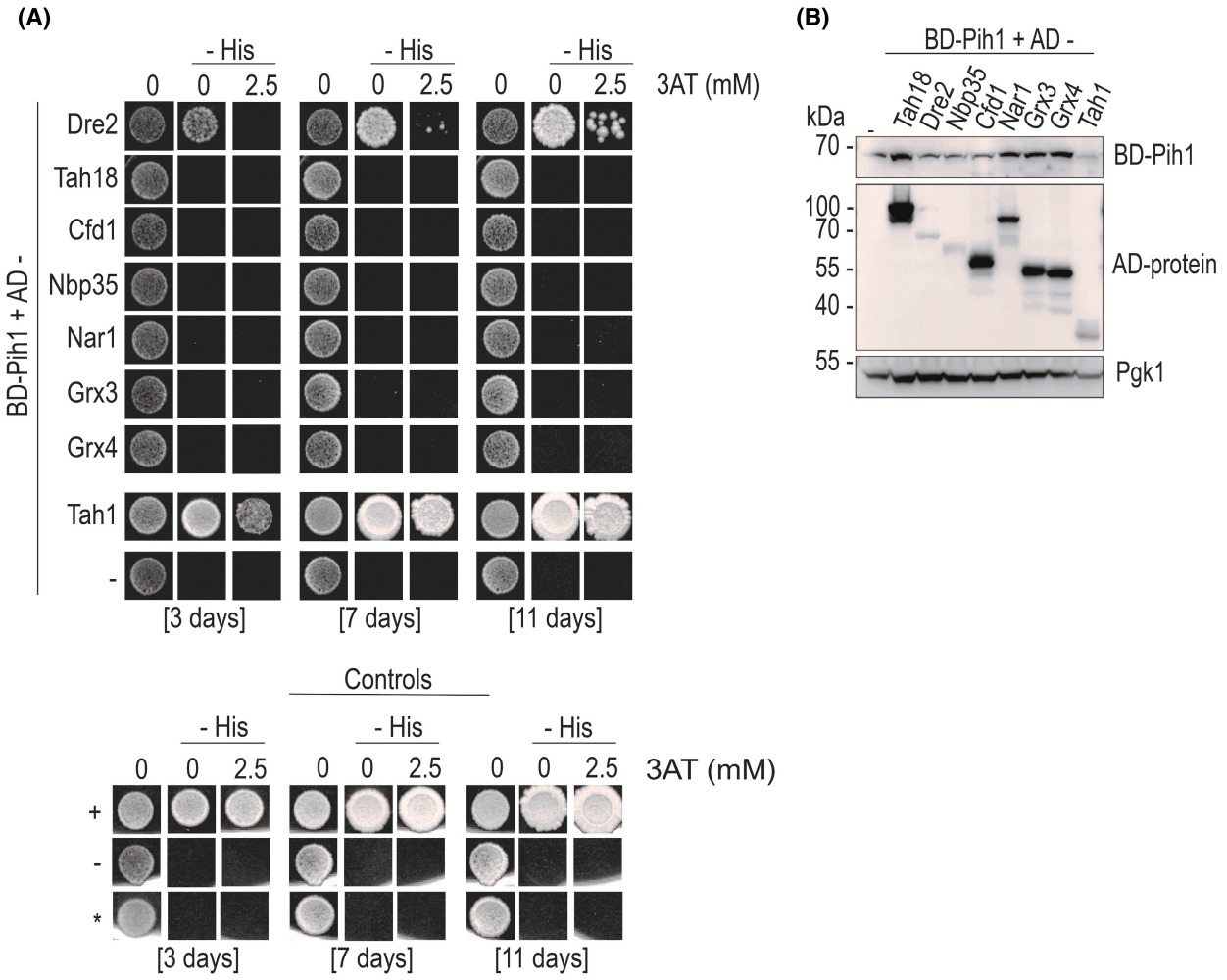

Fig. 1. The Hsp90 co-chaperone Pih1 interacts with the CIA protein Dre2 in Y2H assays. (A) Top: The indicated CIA proteins and Tah1 (a known Pih1 interactor) were fused to the Gal4-AD (Activation Domain), and Pih1 was fused to the Gal4-DNA-BD (Binding Domain). Histidine-based prototrophic recovery was used to select for positive interactions. 2.5 mM 3-amino-1,2,4-triazole (3AT) served to evaluate the interaction strength. Cells spots were photographed after the indicated time points. Tah1-AD, positive control; –, negative control, BD-Pih1 + AD. Bottom: Validation of the Y2H system with controls supplied by the manufacturer. +, BD-53 + AD-T (positive control); –, BD-Lamin + AD-T (negative control), and *, BD + AD (additional negative control). These cultivations were done on SD agar plates, lacking histidine where indicated, followed by incubation at 30 °C for the indicated days. (B) Cell extracts from the cells of part A were subjected to immunostaining of the indicated antigens to confirm the expression of the fusion proteins used in the Y2H assay. Cytosolic Pgk1 was used as a loading control, and molecular mass markers are on the left.

was used to screen for positive interactors. Of the CIA proteins tested, only the strain harboring the AD-Dre2 construct rescued growth in the absence of histidine, indicating a robust interaction. The Dre2-Pih1 interaction-dependent growth was abrogated upon the addition of 2.5 mM 3-amino-1,2,4-triazole (3AT), a competitive inhibitor of the *HIS3* gene product, suggesting a transient and weak interaction (Fig. 1A, top). This interaction, together with the numerous interactions described previously (see Introduction; Fig. S1), led us to hypothesize a role for the Hsp90 chaperone system in the CIA pathway and/or iron regulation. We therefore investigated the potential impact of deficiencies in Pih1 or Hsp90 on these processes.

Analysis of Fe/S protein biogenesis in Pih1- and Hsp90-deficient yeast strains

To understand the functional importance of the Dre2-Pih1 interaction, we created two conditional *S. cerevisiae* strains by PCR-mediated gene replacement in which the endogenous promoter of *PIH1* was replaced by the glucose-repressible, galactose-inducible *GAL-L* or *GAL1* promoters (Table S1; Fig. S2A–D;

W303-1B background). Despite efficient depletion of Pih1, enzyme activities of the cytosolic Fe/S proteins isopropyl malate isomerase (Leu1) and sulfite reductase (SiR), as well as the mitochondrial Fe/S protein aconitase (Aco) were not affected (Fig. S2A–C). SiR activity was tested using a plate-based assay that relies on the formation of a brown bismuth sulfide-containing precipitate in cells that contain holo-SiR activity [34,53]. Consistently, the expression of the *FET3* promoter remained at wild-type levels, even after 64 h of depletion in both strains (Fig. S2D). *FET3* is a member of the yeast iron regulon, a set of genes involved in iron metabolism that are regulated by the iron-responsive transcription factors Aft1 and Aft2. They are induced upon iron starvation or Fe/S protein biogenesis defects, in particular upon depletion of the early components of the mitochondrial ISC system or the ABC transporter Atm1 (Fig. S2D, right; Fig. S1) [55,56]. We also used the deletion strain *pih1Δ* (BY4742 background) to test the enzyme activities of several Fe/S enzymes. Aconitase and sulfite reductase activities were hardly affected, and Leu1 activity was reduced by 46% (Fig. S2E,F). This Leu1 activity defect was likely not a Fe/S cluster-related consequence, as the activities of the other Fe/S proteins remained at wild-type levels, and Leu1 activity was unchanged upon efficient depletion of Pih1 in the Gal-strains (W303-1B background; Fig. S2B,C).

As Pih1 is a nonessential protein in *S. cerevisiae*, its role might be bypassed *in vivo*. Hence, to more generally investigate the involvement of the Hsp90 chaperone system in cellular Fe/S protein biogenesis, we created a *S. cerevisiae* strain conditionally expressing the Hsp90 chaperone. *S. cerevisiae* encodes two cytosolic Hsp90 isoforms, the constitutive Hsc82 and the heat-shock-inducible Hsp82 [28–30,57]. Expression of one isoform is sufficient and necessary for cell viability under both heat-shock and non-heat-shock conditions. To create a strain suitable for critical Hsp90 depletion, we exchanged the endogenous promoter of *HSC82* by a glucose-repressible, galactose-inducible *GAL-L* promoter employing PCR-mediated gene replacement in a *hsp82Δ* deletion strain background. In the resulting Gal-HSC82/hsp82Δ strain (Gal-c82p82Δ), efficient depletion of Hsc82 protein upon growth in glucose-containing minimal medium was confirmed by immunostaining (Fig. 2A and Fig. S3A). As expected, Hsc82-depleted Gal-c82p82Δ cells displayed a growth defect, in particular when incubated at 37 °C or 42 °C (Fig. S3B) [30,57]. Moreover, after 30 h of Hsc82 depletion, the viability of these cells tested on a galactose-containing medium was severely compromised, confirming the essential role of Hsp90 *in vivo* (Fig. S3C).

We next analyzed the effect of Hsp90 depletion on the levels of certain CIA factors and iron-regulating proteins as suspected Hsp90 clients (see Introduction; Fig. S1). The levels of Dre2, Nbp35, and Grx4 were not compromised after Hsc82 depletion for 30 h, and only a moderate decrease in Nbp35 was observed after 40 h depletion (Fig. 2A), suggesting a minor dependence of these proteins on Hsp90 chaperoning *in vivo*. More importantly, the enzyme activity of the Fe/S cluster-containing protein Leu1 was not affected after Hsc82 depletion for 30 or 40 h (Fig. 2B). Likewise, the activity of a second cytosolic Fe/S enzyme, sulfite reductase was unchanged upon Hsp90 deficiency (Fig. 2C). Colonies of Hsc82-depleted Gal-c82p82Δ cells displayed the same brownish color as wild-type cells or cells grown under Hsc82-inducing conditions (Fig. 2C, top). When Gal-c82p82Δ cells were precultured in a glucose-containing minimal medium for 10 h before plating, a slight growth defect became apparent. Yet, SiR activity was still not severely compromised, as the colonies remained brownish, with a difference in color tone that correlated well with their attenuated growth (Fig. 2C, bottom). By contrast, colonies of Gal-*DRE2*, a Gal-promoter exchange mutant of the CIA factor Dre2 [58] remained white when cultivated on a glucose-containing medium (Fig. 2D). Together, these findings did not indicate a critical cytosolic Fe/S protein defect upon Pih1 or Hsp90 depletion.

Apoproteins might undergo conformational changes upon Fe/S cluster insertion. We therefore investigated the possibility that Hsp90 chaperone activity might influence the *de novo* Fe/S cluster insertion into apoproteins by using an *in vivo* ^{55}Fe radiolabeling assay in yeast [50,52]. ^{55}Fe/S target proteins were immunoprecipitated with specific antibodies and the associated radioactivity was estimated by scintillation counting. We chose Leu1 and the Pih1 interactor Dre2 (see Fig. 1A) for analysis, as these Fe/S proteins can be followed at endogenous expression levels without overproduction. ^{55}Fe incorporation into Leu1 was unaffected in Gal-c82p82Δ after 30 h of Hsc82 depletion, and, surprisingly, Dre2 showed even a twofold increase in ^{55}Fe binding compared with the control (Fig. 2E). The latter result correlated with slightly increased Dre2 levels observed in total extracts after ^{55}Fe incorporation (Fig. 2F). This behavior is slightly different from that seen in Fig. 2A, and possibly caused by the different growth conditions; *in vivo* ^{55}Fe radiolabeling involves prior growth in the iron-poor medium. Hence, Dre2 levels might be slightly influenced by the conditions prevailing upon the shift of the Gal-c82p82Δ cells to glucose medium with or without iron.

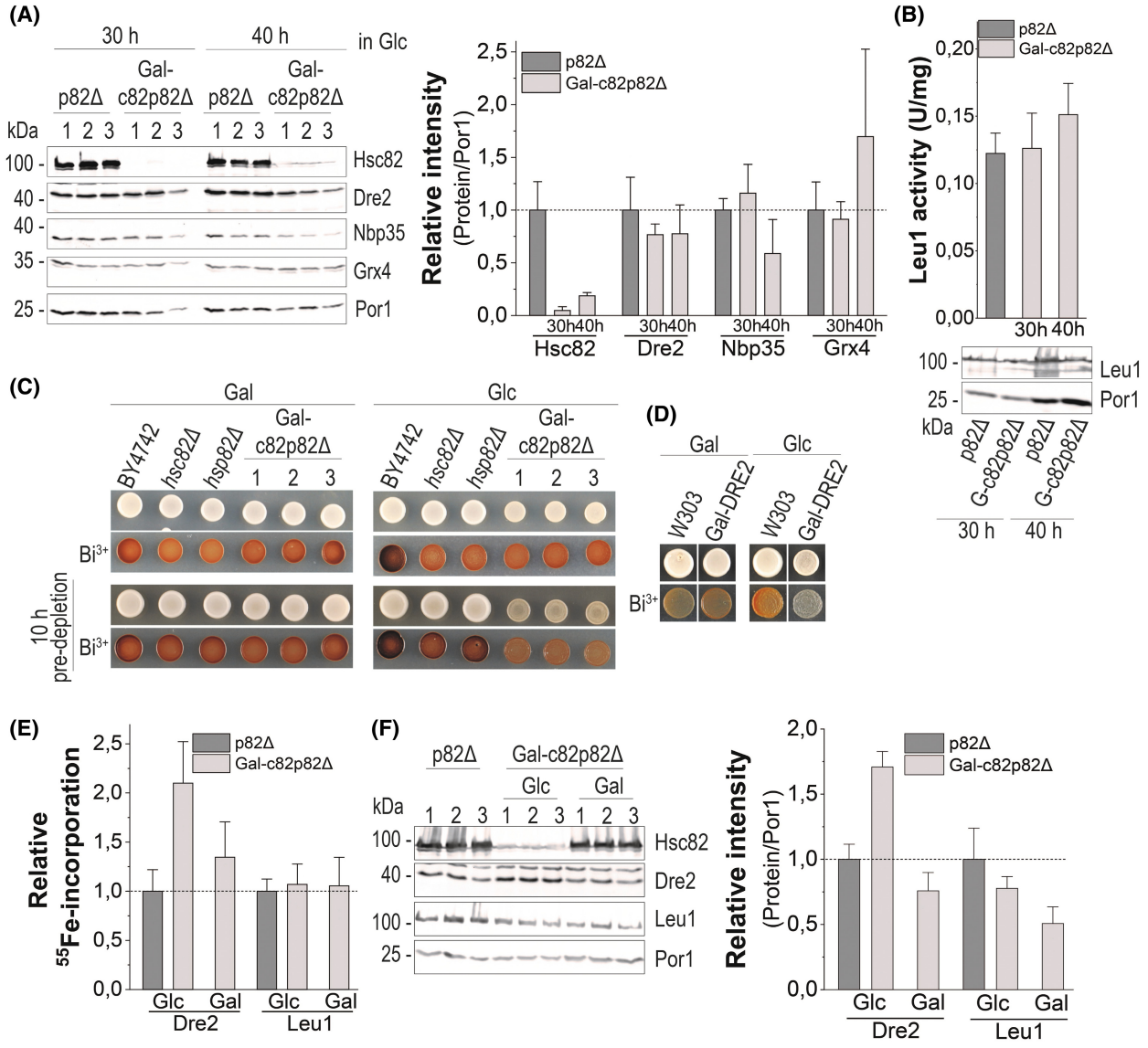

Fig. 2. Hsp90 depletion does not affect cytosolic Fe/S protein maturation. (A) Left: The indicated cells were grown in SD liquid medium for 30 or 40 h. Clarified extracts were subjected to immunostaining of the indicated CIA proteins. Porin (Por1) served as a loading control. Right: Quantification of the immunostaining shown on the left. For the p82Δ strain and both time points the mean ratio protein/Por1 was determined and each protein set to 1. For the Gal-c82p82Δ strain the protein/Por1 ratios at 30 and 40 h were determined individually and normalized to the respective p82Δ mean value. Error bars indicate the SD ($n \geq 3$). (B) Top: Leu1 enzyme activity measured in cell extracts of the indicated strains after 30 or 40 h of growth in SD liquid medium. For the p82Δ cells the values recorded at 30 and 40 h were grouped together. Error bars indicate the SD ($n \geq 3$). Bottom: immunostaining of Leu1 and porin (Por1). (C) Sulfite reductase (SiR) activity was measured by a plate assay based on the SiR activity-dependent formation of a brown bismuth sulfide-containing precipitate. The indicated strains were spotted onto standard or Bi^{3+}-glucose (Glc)- or -galactose (Gal)-containing minimal medium agar plates, and incubated at 30 °C for 3 days (top). To predeplete Hsc82, all strains were grown for 10 h in SD liquid medium before plating and analysis as above (bottom). (D) As a control, SiR activities were measured for wild-type and Gal-DRE2 cells (W303-1A background) as described in part (C). (E) p82Δ and Gal-c82p82Δ cells were cultivated in iron-poor minimal medium supplemented with Glc or Gal as indicated for 30 h. After *in vivo* ^{55}Fe radiolabeling, endogenous Leu1 or Dre2 were immunoprecipitated with antibodies against these proteins. ^{55}Fe associated to the immunobeads was quantified by scintillation counting. The mean ^{55}Fe per gram of wet cells (3600 cpm·g^{-1} for Leu1 and 7400 cpm·g^{-1} for Dre2) for strain p82Δ was set to 1 for each experiment. Error bars indicate the SD ($n = 6$). (F) Left: The total extracts used for immunoprecipitation after ^{55}Fe incorporation were subjected to immunostaining of the indicated proteins. Porin (Por1) was used as a loading control. Right: Quantification of the immunostaining shown on the left. The mean ratio protein/Por1 for the p82Δ strain was set to 1 for each experiment. Error bars indicate the SD ($n = 3$). Representative blots are shown. p82Δ, *hsp82Δ*; Gal-c82p82Δ, Gal-L-HSC82/hsp82Δ; 1,2,3, biological replicates.

We further investigated the influence of Hsp90 on iron homeostasis, because of the multiple links between this chaperone and proteins involved in iron regulation (see Introduction; Fig. S1). When Gal-c82p82Δ cells were grown in the glucose-containing minimal medium for 30 h supplemented with ferric ammonium citrate (+Fe) to assure iron sufficiency, the activity of the Aft1-dependent *FET3* promoter remained at basal levels similar to control cells (Fig. 3A). When, however, Gal-c82p82Δ cells were cultivated under iron-depriving conditions in the presence of bathophenanthroline (−Fe), *FET3* expression was stimulated about 8-fold, demonstrating that the Hsp90-depleted cells maintained their physiological response to iron limitation. Collectively, these results do not provide any evidence for a critical role of Hsp90 in cytosolic Fe/S protein assembly or maintenance, nor does Hsp90 deficiency detectably affect the iron regulon.

Since the mitochondrial ISC system plays an important role in the physiological response to iron limitation in eukaryotes, we analyzed the mitochondrial Fe/S protein aconitase. Surprisingly, the activities of the ISC target aconitase and the mitochondrial non-Fe/S enzyme malate dehydrogenase (MDH) as a control were more than 3.5-fold upregulated upon Hsc82 depletion (Fig. 3B). To gain a better view into how mitochondria respond to low levels of Hsp90, we further measured citrate synthase (CS) and respiratory complex IV (cytochrome *c* oxidase, COX) activities, which were also more than 4- and 1.6-fold upregulated, respectively (Fig. 3B). Apparently, although Hsp90 is essential for viability, the general fitness of mitochondria is improved upon Hsp90 depletion. Intriguingly, the global list of upregulated proteins in Hsp90-depleted cells includes several subunits of the respiratory chain complexes II (four subunits), III (seven subunits), and IV (nine subunits) [35]. Further, the entire F_1F_o-ATP synthase (13 components), four proteins of ubiquinone (CoQ_6) biosynthesis, and at least four enzymes of the TCA cycle were upregulated. The sum of these findings strongly suggests that *S. cerevisiae* responds to Hsp90 deficiency by upregulating mitochondrial metabolism including oxidative phosphorylation.

Overall, our results on Pih1- and Hsp90-deficient yeast cells did not reveal any primary function of the Hsp90 chaperone system for cellular Fe/S protein biogenesis or iron regulation, despite numerous, apparently indirect links between the two processes. Our data do not exclude a nonessential role of Hsp90 in these processes, but such a function would be maintained with minimal amounts of the chaperone.

The essential cytosolic Ydj1 does not play a critical role in iron-dependent processes

In *Arabidopsis thaliana*, two related DnaJ-like co-chaperones, DJA5 and DJA6 (86% sequence identity), have been implicated as dedicated iron donors for the SUF system, the Fe/S protein assembly system in plastids [39]. Both DJA5 and DJA6 were shown *in vivo* and *in vitro* to bind iron *via* a cysteine-rich zinc-finger-

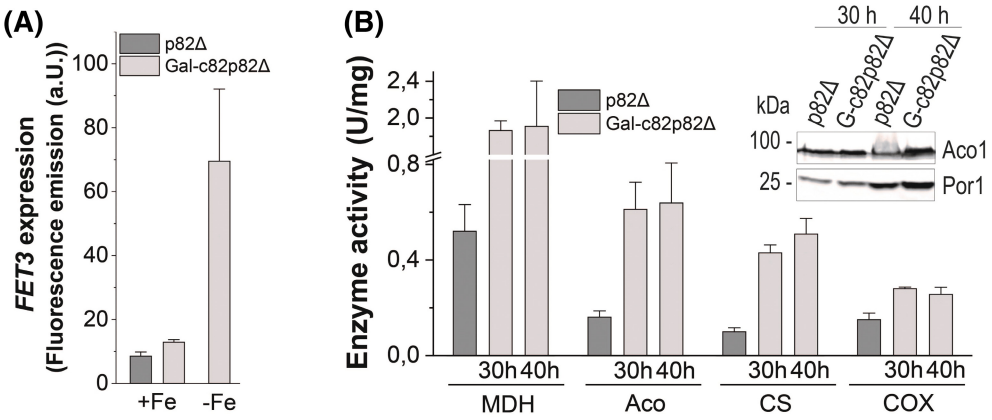

Fig. 3. Hsp90 depletion has no effect on cellular iron regulation but upregulates mitochondrial metabolism-related enzymes. (A) The yeast strains p82Δ and Gal-c82p82Δ were transformed with plasmid pFET3-GFP, and cells were cultivated for 30 h in SD liquid medium supplemented with 50 μM ferric ammonium citrate (+Fe) or 50 μM bathophenanthroline (−Fe). The GFP-specific fluorescence emission was recorded. Error bars indicate the SD ($n = 3$). (B) Malate dehydrogenase (MDH), aconitase (Aco), citrate synthase (CS) and respiratory complex IV (cytochrome *c* oxidase, COX) activities were measured in cell extracts of the indicated strains after 30 or 40 h of growth in SD liquid medium. For the p82Δ cells the values recorded at 30 and 40 h were grouped together. Error bars indicate the SD ($n \geq 3$). Insert: Cell extracts were used for immunostaining of aconitase (Aco1) and porin (Por1). Representative blots are shown.

like region (ZFLR) composed of four conserved CxxCxGxG motifs that distinguish these proteins from most other members of the Hsp40 co-chaperone family (Fig. S4A,B). As noted above, the mitochondrial ISC machinery depends on the function of the dedicated J-protein Jac1, which, however, does not contain a ZFLR, and is not implicated in iron binding. We employed the yeast model to investigate whether eukaryotes might contain DJA5-DJA6-like specialized Hsp40 proteins in the cytosol or mitochondria with an iron-donor function for cellular Fe/S protein biogenesis. *S. cerevisiae* encodes five Hsp40-like proteins with a central ZFLR similar to that in DJA5-DJA6, termed Ydj1 (human DNAJA1), Mdj1 (human DNAJA3), Xdj1 (human DNAJA2, DNAJA4), as well as Scj1 and Apj1 (both lacking a human homolog) [41] (Fig. S4A,B). The overall sequence identity among these proteins and with DJA5-DJA6 is rather low (around 30%), yet both the N-terminal J domain and particularly the ZFLR are well conserved and have been defined structurally (Fig. S4A,C,D). Ydj1 is located in the cytosol and may be a good iron-donor candidate for the CIA system because it is essential for cell viability similar to most CIA factors [59]. Mdj1 is located in the mitochondrial matrix and its deletion results in loss of respiratory function, which makes the protein a good candidate for an iron donor within the mitochondrial ISC system [60,61]. Xdj1 is attached to the mitochondrial outer membrane and to the nucleus [62,63], while Apj1 localizes to cytosol, mitochondria, and the nucleus. Gene deletion of either *XDJ1* or *APJ1* is not associated with severe phenotypical consequences making a critical function within the essential cytosolic Fe/S protein biogenesis pathway unlikely [40,64]. Finally, Scj1 is located within the endoplasmic reticulum, and hence can be excluded as an iron-donor candidate, since this compartment is not known to contain Fe/S proteins. Based on these considerations, we concentrated our analyses on Ydj1 and Mdj1.

For the investigation of the potential involvement of cytosolic Ydj1 in Fe/S protein biogenesis, we created a *GAL-L*-promoter exchange mutant by PCR-mediated gene replacement. Consistent with the essential character of *YDJ1*, the resulting Gal-YDJ1 strain showed a growth arrest under repressing conditions on glucose-containing medium (Fig. 4A). However, both the protein levels and enzyme activities of the cytosolic Fe/S protein Leu1 as well as ^{55}Fe binding to Leu1 (measured by the radiolabeling-immunoprecipitation assay described in Fig. 2E) did not decrease in Gal-YDJ1 cells upon Ydj1 depletion (Fig. 4B–D). Interestingly, Leu1 activity even increased after longer depletion times. The same was observed for the enzyme activity of mitochondrial aconitase (Fig. 4C). As a sensitive readout of defects in Fe/S protein biogenesis, we measured the expression of *FET3*, yet no differences to wild-type levels were found for *FET3* expression after 48 h of Ydj1 depletion (Fig. 4E). Together, our findings do not provide any evidence for a direct important role of Ydj1 in cytosolic Fe/S protein maturation or in the iron supply of mitochondria.

Ydj1 has been implicated in the function of ribonucleotide reductase by playing a role in the stability of Rnr2, its iron co-factor binding subunit [65]. Consistent with this observation, Ydj1-depleted Gal-YDJ1 cells displayed slightly reduced levels of Rnr2 (Fig. 4B). However, ^{55}Fe binding to Rnr2 even increased threefold in Gal-YDJ1 cells under Ydj1-depleting conditions, suggesting that the observed defects in ribonucleotide reductase were not due to impaired iron loading (Fig. 4D). Taken together, these results do not provide any evidence for a direct role of Ydj1 in iron regulation or in iron donation to cellular Fe/S protein biogenesis or ribonucleotide reductase.

Mitochondrial Mdj1 does not play a role in Fe/S protein assembly and iron regulation

For the investigation of Mdj1 as a potential iron chaperone, we created both deletion and *GAL-L*-promoter exchange mutants by PCR-mediated gene replacement in both W303-1A and BY4742 yeast strain backgrounds. As expected, the resulting *mdj1*Δ and Gal-MDJ1 strains failed to grow under respiratory growth conditions in the presence of glycerol (Figs S5A,D and S6A). In these strains, Mdj1 was either absent or severely depleted in mitochondrial extracts, respectively (Figs S5B and S6B). Using a rho^0 (no mitochondrial DNA) tester strain, we confirmed the expected loss of mitochondrial DNA in the W303-1A *mdj1*Δ strain [66] (Fig. S5C). Nevertheless, protein levels of aconitase and the ISC factors Isu1 and Isa1 were not deceased in W303-1A Gal-MDJ1 cells under Mdj1-depleting conditions (Fig. 5A). In both strain backgrounds (W303-1A and BY4742), enzyme activities of mitochondrial aconitase and cytosolic Leu1 were at wild-type or even higher levels in *mdj1*Δ cells or Gal-MDJ1 cells after 40 h of depletion (Fig. 5B and Fig. S6C). Consistently, ^{55}Fe incorporation into mitochondrial aconitase or cytosolic Leu1 remained unaffected in the W303-1A *mdj1*Δ strain (Fig. 5C). The expression of the yeast iron uptake gene *FET3* was not increased upon Mdj1 depletion or deletion in the W303-1A strain background, in contrast to deficiency of the ISC factor Grx5 as a control (Fig. 5D). These data indicated that mitochondrial Fe/

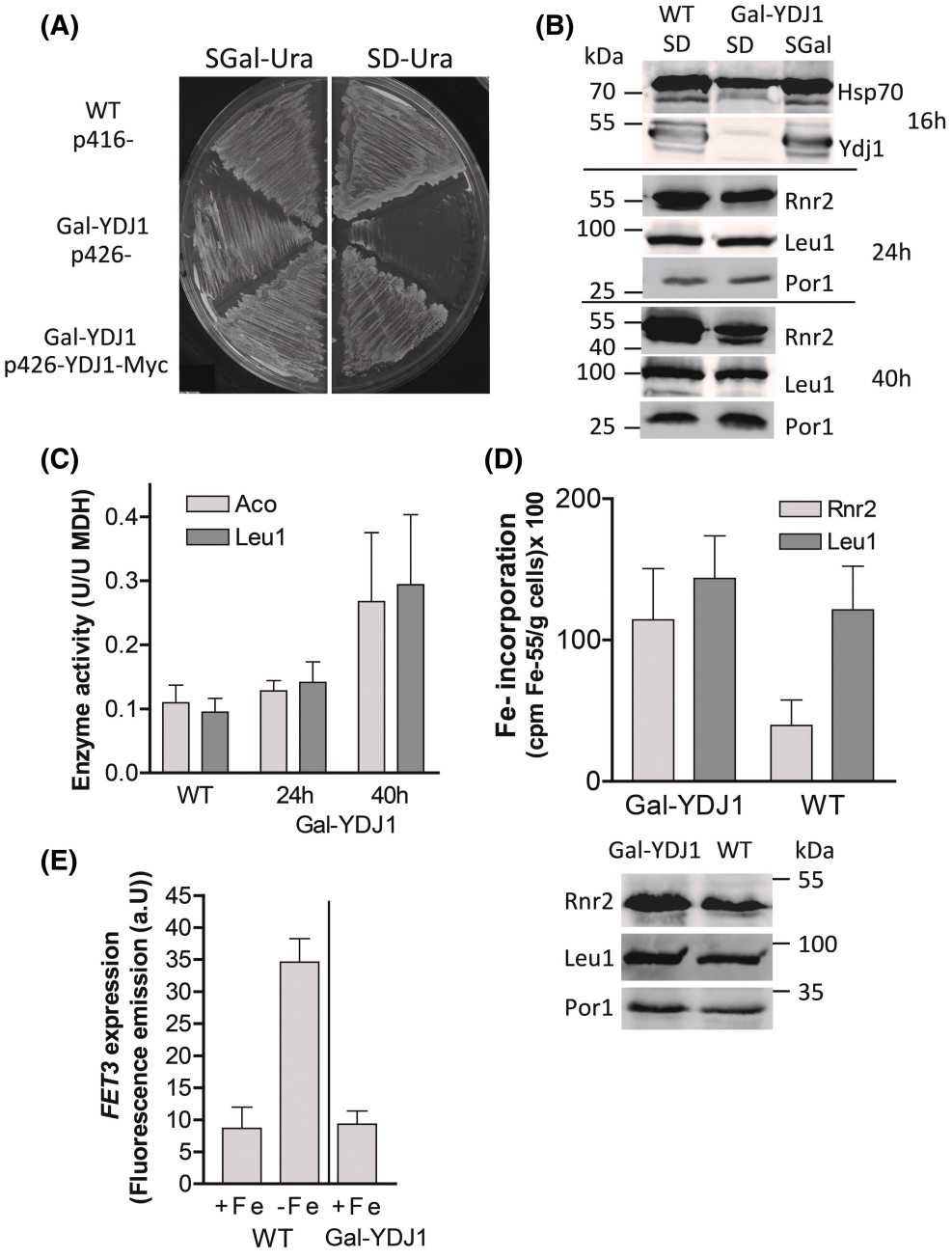

Fig. 4. Testing the role of Ydj1 in cellular Fe/S protein maturation and iron regulation. (A) Gal-YDJ1 cells plasmid-expressing the fusion protein YDJ1-Myc or the empty vector were cultivated on minimal medium agar plates supplemented with galactose (SGal) or glucose (SD) for 40 h at 30 °C. Wild-type (WT) cells (W303-1A) served as a control. (B, C) WT and Gal-YDJ1 cells were cultivated in SD or SGal liquid medium for 16, 24 and 40 h, as indicated. Cell extracts were analyzed for the levels of the indicated proteins by immunoblotting (B), and the enzyme activities of aconitase (Aco) and Leu1 (C). (D) WT and Gal-YDJ1 cells were cultivated in iron-poor SD liquid medium for 48 h, and ^{55}Fe binding to Leu1 and ribonucleotide reductase subunit 2 (Rnr2) were determined by radiolabeling and immunoprecipitation with specific antibodies. The lower panel shows the presence of the precipitated proteins by immunostaining, using porin as a loading control. (E) WT and Gal-YDJ1 cells plasmid-expressing FET3-GFP were cultivated in SD liquid medium supplemented with 50 μM ferric ammonium citrate (+Fe) for 48 h. The GFP-specific fluorescence emission of whole cells was recorded. WT cells cultivated in the presence of 50 μM bathophenanthroline (−Fe) served as a control for *FET3* activation. Error bars indicate the SD ($n \geq 4$).

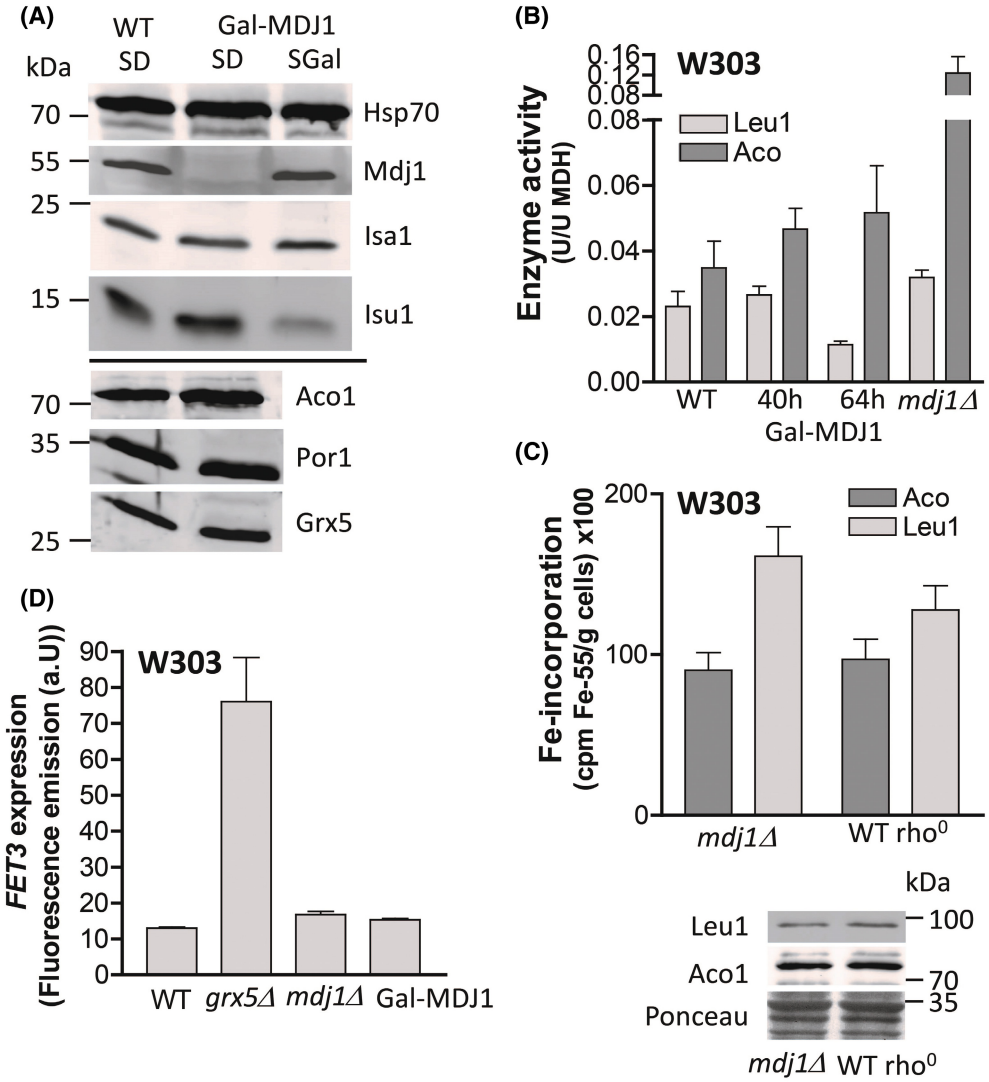

Fig. 5. Testing the role of Mdj1 in cellular Fe/S protein maturation and iron regulation. (A) Cell extracts of wild-type (WT) and Mdj1-depleted Gal-MDJ1 cells (W303-1A background) were analyzed for the levels of the indicated proteins by immunoblotting. Gal-MDJ1 cells were depleted of Mdj1 by growth in SD medium for 40 h prior to analysis. (B) Enzyme activities of aconitase (Aco) and Leu1 were determined in cell extracts of the indicated strains. (C) Wild-type (WT rho^0) and mdj1Δ cells were cultivated in iron-poor SD liquid medium and ^{55}Fe incorporation into Leu1 and aconitase (Aco) was determined by radiolabeling and immunoprecipitation with specific antibodies. Lower panel: Expression levels of the precipitated proteins were assessed by immunostaining. Unspecific bands from Ponceau staining served as a loading control. (D) The indicated strains plasmid-expressing FET3-GFP were cultivated in SD liquid medium supplemented with 50 μM ferric ammonium citrate, and the GFP-specific fluorescence emission was recorded. *grx5*Δ cells served as a control for constitutive activation of the *FET3* gene. Error bars indicate the SD ($n \geq 3$).

S protein biogenesis remained unaffected in the absence of Mdj1. Surprisingly, in the BY4742 background strains a partial induction of *FET3* was observed upon Mdj1 deficiency (Fig. S6D). Since mitochondrial Fe/S protein assembly was unaffected (Fig. S6C), this effect was likely indirect. Taken together, our findings do not provide evidence for a critical role of Mdj1 as an iron chaperone for mitochondrial Fe/S protein biogenesis, as described for DJA5-DJA6 in plastids from *A. thaliana*.

No detectable *in vivo* iron binding to Ydj1 and Mdj1

We finally examined iron binding to yeast Mdj1 and Ydj1. *In vivo* iron binding was followed by employing

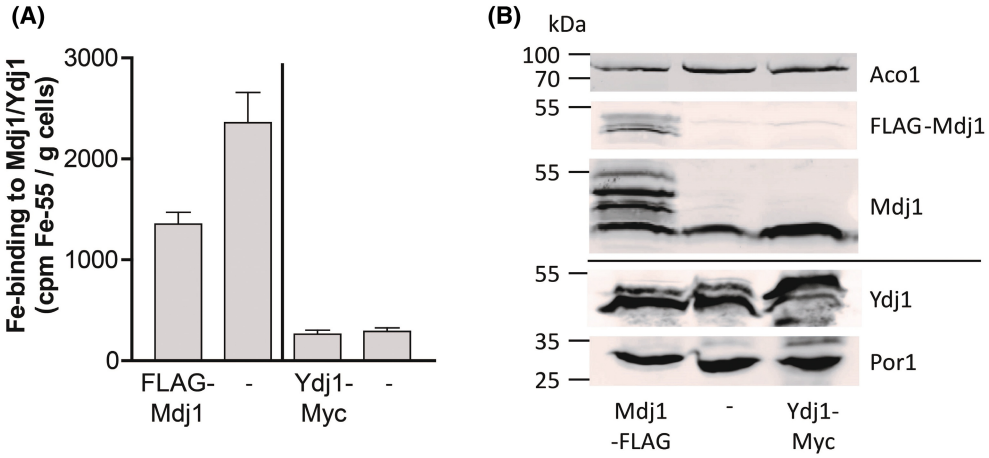

Fig. 6. Both Ydj1 and Mdj1 do not specifically bind iron *in vivo*. Wild-type cells (W303-1A) harboring plasmid pYES-FLAG-MDJ1 and Gal-YDJ1 cells harboring plasmid p426-YDJ1-Myc were cultivated in iron-poor SGal or SD liquid medium, respectively, for 40 h. (A) ^{55}Fe incorporation into FLAG-Mdj1 or Ydj1-Myc was determined by radiolabeling and immunoprecipitation with α-FLAG and α-Myc-immunobeads, respectively. Wild-type cells harboring the empty vector (–) served as a control for background ^{55}Fe binding observed with the different antibodies. Error bars indicate the SD ($n > 4$). (B) The expression of the precipitated proteins was tested by immunostaining with antibodies against FLAG, Mdj1 and Ydj1 using Aco1 and porin (Por1) as loading controls.

the ^{55}Fe radiolabeling-immunoprecipitation assay (cf. Fig. 2E). For this purpose, we generated high-copy vectors for the overproduction of tagged proteins, namely FLAG-Mdj1 and Ydj1-Myc (Fig. 4A, Table S2). Upon ^{55}Fe radiolabeling and subsequent affinity precipitation, less than background levels of radioactivity were associated with overproduced FLAG-Mdj1 in wild-type cells (Fig. 6A, left). Likewise, no ^{55}Fe above background was associated with overproduced Ydj1-Myc (Fig. 6A, right). In both cases, the tagged proteins were expressed well (Fig. 6B). This lack of *in vivo* ^{55}Fe binding to both Ydj1 and Mdj1 nicely fits to the independence of cellular Fe/S protein biogenesis and the associated iron regulation from these two ZFLR-containing yeast J-proteins.

In vitro iron binding could be tested only for Ydj1 because purified Mdj1 was instable and precipitated. Recombinant His-tagged Ydj1 surprisingly displayed a reddish-brown color after purification from *E. coli* extracts (Fig. S7). The spectrum of the purified protein showed absorption bands at 360 and 480 nm, features reminiscent of those of DJA5-DJA6 from *A. thaliana* [39]. In order to explore whether Ydj1 may accommodate mononuclear iron or Fe/S clusters, the protein was incubated with $FeCl_2$, or subjected to a Fe/S cluster reconstitution protocol (Fe^{3+}-ammonium citrate plus Li_2S for 3 h under anaerobic conditions). Only background amounts of acid labile sulfide were detected in Ydj1 after Fe^{3+} and sulfide treatment, essentially excluding that Ydj1 may accommodate Fe/S clusters (Fig. S7B). Fe^{2+} treatment slightly intensified the color of as purified Ydj1, yielding sub-stochiometric amounts of bound iron (~ 0.6 ions per protein). We conclude that Ydj1, upon ectopic expression in *E. coli*, can bind iron, yet our inability to detect both iron binding *in vivo* and iron-related phenotypes in Ydj1-depleted cells argues against a physiological relevance of these *in vitro* findings. The situation is radically different from the studies with plastidial DJA5-DJA6 where iron binding was observed both *in vivo* and *in vitro*, and DJA5-DJA6 depletion was associated with strong effects on, e.g., plastidial Fe/S protein assembly [39]. Collectively, we conclude that Ydj1 and Mdj1, in contrast to *A. thaliana* DJA5-DJA6, use Zn rather than Fe in the ZFLR for their chaperone activity, as found in the crystal structure of Ydj1 [67].

Conclusions

Numerous systematic genetic and physical interaction studies have suggested a functional link between the essential Hsp90 chaperone system and both cellular Fe/S protein biogenesis and iron regulation. In our current study, we found no *in vivo* evidence in the *S. cerevisiae* model system for a crucial physiological connection of these pathways under standard growth conditions. Depletion of Pih1 or Hsp90 to physiologically critical levels in yeast cells did not affect these iron-related processes. While our findings do not rule out an auxiliary function of Pih1 and Hsp90 in these

processes, it is obvious that other pathways depend more critically on the chaperones. Interestingly, the abundance and activity of numerous mitochondrial proteins relevant for (iron-dependent) metabolism and respiration were upregulated in Hsp90-depleted cells, an observation that deserves future experimental attention.

Moreover, we found no direct crucial roles of the Hsp70-interacting DnaJ-proteins Ydj1 and Mdj1 in cellular Fe/S protein maturation or iron regulation *in vivo*. Although Ydj1 and Mdj1 contain a conserved ZFLR similar to that required for *in vivo* and *in vitro* iron binding to the DnaJ-like iron chaperones DJA5-DJA6 in plastids of *A. thaliana* [39], we did not detect any iron associated with Ydj1 and Mdj1 *in vivo*, consistent with the lack of iron-related phenotypes upon Ydj1 and Mdj1 deficiencies. Nevertheless, purified Ydj1 was able to bind sub-stochiometric levels of iron upon ectopic bacterial expression reiterating in principle the ability of the ZFLR to coordinate this metal. However, our *in vivo* findings provide clear evidence that in the native environment, the ZFLR of Ydj1 may be loaded with zinc rather than iron, as originally proposed [67]. Therefore, future studies exploring the molecular basis of the striking metal specificity of DJA5-DJA6 (for Fe) versus other ZFLR-containing J-proteins (for Zn) may have to be carried out in the respective native compartments of the studied J-proteins. Since both protein subclasses contain highly similar ZFLR domains with no conspicuous structural differences, such studies may even lead to the discovery of dedicated metal chaperones assisting the specific insertion of the physiologically desired metal ion.

Acknowledgements

We thank Dr Walid A. Houry (Toronto) for the kind gift of anti-Hsp90 and anti-Pih1, Dr Dejana Mokranjac (Munich) for anti-Mdj1, Dr Johannes Buchner (Munich) for anti-Ydj1, Dr Fernando Gonzales-Zubiate (Sao Paulo) for carrying out the large-scale Y2H-based mapping of Pih1 interactors, and Jonas Göthe (Marburg) for initial experiments on Ydj1 expression. We acknowledge the contribution of the Core Facility 'Protein Biochemistry and Spectroscopy' of Philipps-Universität Marburg. We gratefully acknowledge generous financial funding from Fundação de Amparo à Pesquisa do Estado de São Paulo (FAPESP) to CCO (2020/00901-1) and to FAC (2019/00527-5 and 2021/06497-0), as well as from Deutsche Forschungsgemeinschaft to RL (Koselleck grant LI 415/6 and SPP 1927, LI 415/7). Open Access funding enabled and organized by Projekt DEAL.

Author contributions

FAC and UM contributed to conceptualization, data acquisition, data analysis, and writing of the original draft. JJB, VR, and MS contributed to data acquisition and analysis. CCO and RL contributed to conceptualization, data analysis, funding acquisition, project supervision, and writing of the manuscript.

Peer Review

The peer review history for this article is available at https://www.webofscience.com/api/gateway/wos/peer-review/10.1002/1873-3468.14612.

Data accessibility

The data that support the findings of this study are available from the joint first authors and the joint senior authors upon reasonable request.

References

1 Zanello P (2019) Structure and electrochemistry of proteins harboring iron-sulfur clusters of different nuclearities. Part IV. Canonical, non-canonical and hybrid iron-sulfur proteins. *J Struct Biol* **205**, 103–120.
2 Braymer JJ, Freibert SA, Rakwalska-Bange M and Lill R (2021) Mechanistic concepts of iron-sulfur protein biogenesis in biology. *Biochim Biophys Acta Mol Cell Res* **1868**, 118863.
3 Lill R (2020) From the discovery to molecular understanding of cellular iron-sulfur protein biogenesis. *Biol Chem* **401**, 855–876.
4 Lill R and Freibert SA (2020) Mechanisms of mitochondrial iron–sulfur protein biogenesis. *Annu Rev Biochem* **89**, 471–499.
5 Maio N, Jain A and Rouault TA (2020) Mammalian iron-sulfur cluster biogenesis: recent insights into the roles of frataxin, acyl carrier protein and ATPase-mediated transfer to recipient proteins. *Curr Opin Chem Biol* **55**, 34–44.
6 Ciofi-Baffoni S, Nasta V and Banci L (2018) Protein networks in the maturation of human iron-sulfur proteins. *Metallomics* **10**, 49–72.
7 Przybyla-Toscano J, Roland M, Gaymard F, Couturier J and Rouhier N (2018) Roles and maturation of iron-sulfur proteins in plastids. *J Biol Inorg Chem* **23**, 545–566.
8 Baussier C, Fakroun S, Aubert C, Dubrac S, Mandin P, Py B and Barras F (2020) Making iron-sulfur cluster: structure, regulation and evolution of the bacterial ISC system. *Adv Microb Physiol* **76**, 1–39.
9 Paul VD and Lill R (2015) Biogenesis of cytosolic and nuclear iron-sulfur proteins and their role in genome stability. *Biochim Biophys Acta* **1853**, 1528–1539.

10 Garcia PS, Gribaldo S, Py B and Barras F (2019) The SUF system: an ABC ATPase-dependent protein complex with a role in Fe-S cluster biogenesis. *Res Microbiol* **170**, 426–434.
11 Stehling O, Wilbrecht C and Lill R (2014) Mitochondrial iron-sulfur protein biogenesis and human disease. *Biochimie* **100**, 61–77.
12 Beilschmidt LK and Puccio HM (2014) Mammalian Fe-S cluster biogenesis and its implication in disease. *Biochimie* **100**, 48–60.
13 Maio N and Rouault TA (2020) Outlining the complex pathway of mammalian Fe-S cluster biogenesis. *Trends Biochem Sci* **45**, 411–426.
14 Stehling O, Mascarenhas J, Vashisht AA, Sheftel AD, Niggemeyer B, Rösser R, Pierik AJ, Wohlschlegel JA and Lill R (2018) Human CIA2A-FAM96A and CIA2B-FAM96B integrate iron homeostasis and maturation of different subsets of cytosolic-nuclear iron-sulfur proteins. *Cell Metab* **27**, 263.
15 Stehling O, Mascarenhas J, Vashisht AA, Sheftel AD, Niggemeyer B, Rösser R, Pierik AJ, Wohlschlegel JA and Lill R (2013) Human CIA2A-FAM96A and CIA2B-FAM96B integrate iron homeostasis and maturation of different subsets of cytosolic-nuclear iron-sulfur proteins. *Cell Metab* **18**, 187–198.
16 Sheftel AD, Wilbrecht C, Stehling O, Niggemeyer B, Elsasser HP, Muhlenhoff U and Lill R (2012) The human mitochondrial ISCA1, ISCA2, and IBA57 proteins are required for [4Fe-4S] protein maturation. *Mol Biol Cell* **23**, 1157–1166.
17 Kleczewska M, Grabinska A, Jelen M, Stolarska M, Schilke B, Marszalek J, Craig EA and Dutkiewicz R (2020) Biochemical convergence of mitochondrial Hsp70 system specialized in iron-sulfur cluster biogenesis. *Int J Mol Sci* **21**, 3326.
18 Dutkiewicz R and Nowak M (2018) Molecular chaperones involved in mitochondrial iron-sulfur protein biogenesis. *J Biol Inorg Chem* **23**, 569–579.
19 Pukszta S, Schilke B, Dutkiewicz R, Kominek J, Moczulska K, Stepien B, Reitenga KG, Bujnicki JM, Williams B, Craig EA *et al.* (2010) Co-evolution-driven switch of J-protein specificity towards an Hsp70 partner. *EMBO Rep* **11**, 360–365.
20 Uzarska MA, Dutkiewicz R, Freibert SA, Lill R and Muhlenhoff U (2013) The mitochondrial Hsp70 chaperone Ssq1 facilitates Fe/S cluster transfer from Isu1 to Grx5 by complex formation. *Mol Biol Cell* **24**, 1830–1841.
21 Vickery LE and Cupp-Vickery JR (2007) Molecular chaperones HscA/Ssq1 and HscB/Jac1 and their roles in iron-sulfur protein maturation. *Crit Rev Biochem Mol Biol* **42**, 95–111.
22 Maio N, Kim KS, Singh A and Rouault TA (2017) A single adaptable Cochaperone-scaffold complex delivers nascent iron-sulfur clusters to mammalian respiratory chain complexes I–III. *Cell Metab* **25**, 945–953 e6.
23 Kim KS, Maio N, Singh A and Rouault TA (2018) Cytosolic HSC20 integrates de novo iron–sulfur cluster biogenesis with the CIAO1-mediated transfer to recipients. *Hum Mol Genet* **27**, 837–852.
24 Gupta P, Aggarwal N, Batra P, Mishra S and Chaudhuri TK (2006) Co-expression of chaperonin GroEL/GroES enhances in vivo folding of yeast mitochondrial aconitase and alters the growth characteristics of *Escherichia coli*. *Int J Biochem Cell Biol* **38**, 1975–1985.
25 Chaudhuri TK, Farr GW, Fenton WA, Rospert S and Horwich AL (2001) GroEL/GroES-mediated folding of a protein too large to be encapsulated. *Cell* **107**, 235–246.
26 Taipale M, Krykbaeva I, Koeva M, Kayatekin C, Westover KD, Karras GI and Lindquist S (2012) Quantitative analysis of HSP90-client interactions reveals principles of substrate recognition. *Cell* **150**, 987–1001.
27 Taipale M, Jarosz DF and Lindquist S (2010) HSP90 at the hub of protein homeostasis: emerging mechanistic insights. *Nat Rev Mol Cell Biol* **11**, 515–528.
28 Biebl MM and Buchner J (2019) Structure, function, and regulation of the Hsp90 machinery. *Cold Spring Harb Perspect Biol* **11**, a034017.
29 Schopf FH, Biebl MM and Buchner J (2017) The HSP90 chaperone machinery. *Nat Rev Mol Cell Biol* **18**, 345–360.
30 Girstmair H, Tippel F, Lopez A, Tych K, Stein F, Haberkant P, Schmid PWN, Helm D, Rief M, Sattler M *et al.* (2019) The Hsp90 isoforms from *S. cerevisiae* differ in structure, function and client range. *Nat Commun* **10**, 3626.
31 Millson SH, Truman AW, King V, Prodromou C, Pearl LH and Piper PW (2005) A two-hybrid screen of the yeast proteome for Hsp90 interactors uncovers a novel Hsp90 chaperone requirement in the activity of a stress-activated mitogen-activated protein kinase, Slt2p (Mpk1p). *Eukaryot Cell* **4**, 849–860.
32 Kumanovics A, Chen OS, Li L, Bagley D, Adkins EM, Lin H, Dingra NN, Outten CE, Keller G, Winge D *et al.* (2008) Identification of FRA1 and FRA2 as genes involved in regulating the yeast iron regulon in response to decreased mitochondrial iron-sulfur cluster synthesis. *J Biol Chem* **283**, 10276–10286.
33 Zhao R, Davey M, Hsu YC, Kaplanek P, Tong A, Parsons AB, Krogan N, Cagney G, Mai D, Greenblatt J *et al.* (2005) Navigating the chaperone network: an integrative map of physical and genetic interactions mediated by the hsp90 chaperone. *Cell* **120**, 715–727.
34 Paul VD, Mühlenhoff U, Stümpfig M, Seebacher J, Kugler KG, Renicke C, Taxis C, Gavin AC, Pierik AJ and Lill R (2015) The deca-GX3 proteins Yae1-Lto1

function as adaptors recruiting the ABC protein Rli1 for iron-sulfur cluster insertion. *Elife* **4**, e08231.
35 Gopinath RK, You ST, Chien KY, Swamy KB, Yu JS, Schuyler SC and Leu JY (2014) The Hsp90-dependent proteome is conserved and enriched for hub proteins with high levels of protein-protein connectivity. *Genome Biol Evol* **6**, 2851–2865.
36 Lynham J and Houry WA (2022) The role of Hsp90-R2TP in macromolecular complex assembly and stabilization. *Biomolecules* **12**, 1045.
37 Back R, Dominguez C, Rothé B, Bobo C, Beaufils C, Moréra S, Meyer P, Charpentier B, Branlant C, Allain FHT *et al.* (2013) High-resolution structural analysis shows how Tah1 tethers Hsp90 to the R2TP complex. *Structure* **21**, 1834–1847.
38 Munoz-Hernandez H, Pal M, Rodriguez CF, Prodromou C, Pearl LH and Llorca O (2018) Advances on the structure of the R2TP/Prefoldin-like complex. *Adv Exp Med Biol* **1106**, 73–83.
39 Zhang J, Bai Z, Ouyang M, Xu X, Xiong H, Wang Q, Grimm B, Rochaix JD and Zhang L (2021) The DnaJ proteins DJA6 and DJA5 are essential for chloroplast iron-sulfur cluster biogenesis. *EMBO J* **40**, e106742.
40 Walsh P, Bursac D, Law YC, Cyr D and Lithgow T (2004) The J-protein family: modulating protein assembly, disassembly and translocation. *EMBO Rep* **5**, 567–571.
41 Kampinga HH and Craig EA (2010) The HSP70 chaperone machinery: J proteins as drivers of functional specificity. *Nat Rev Mol Cell Biol* **11**, 579–592.
42 Foury F and Roganti T (2002) Deletion of the mitochondrial carrier genes MRS3 and MRS4 suppresses mitochondrial iron accumulation in a yeast frataxin-deficient strain. *J Biol Chem* **277**, 24475–24483.
43 Muhlenhoff U, Stadler JA, Richhardt N, Seubert A, Eickhorst T, Schweyen RJ, Lill R and Wiesenberger G (2003) A specific role of the yeast mitochondrial carriers MRS3/4p in mitochondrial iron acquisition under iron-limiting conditions. *J Biol Chem* **278**, 40612–40620.
44 Froschauer EM, Schweyen RJ and Wiesenberger G (2009) The yeast mitochondrial carrier proteins Mrs3p/Mrs4p mediate iron transport across the inner mitochondrial membrane. *Biochim Biophys Acta* **1788**, 1044–1050.
45 Shaw GC, Cope JJ, Li L, Corson K, Hersey C, Ackermann GE, Gwynn B, Lambert AJ, Wingert RA, Traver D *et al.* (2006) Mitoferrin is essential for erythroid iron assimilation. *Nature* **440**, 96–100.
46 Philpott CC and Jadhav S (2019) The ins and outs of iron: escorting iron through the mammalian cytosol. *Free Radic Biol Med* **133**, 112–117.
47 Philpott CC, Ryu MS, Frey A and Patel S (2017) Cytosolic iron chaperones: proteins delivering iron cofactors in the cytosol of mammalian cells. *J Biol Chem* **292**, 12764–12771.
48 Frey AG, Nandal A, Park JH, Smith PM, Yabe T, Ryu MS, Ghosh MC, Lee J, Rouault TA, Park MH *et al.* (2014) Iron chaperones PCBP1 and PCBP2 mediate the metallation of the dinuclear iron enzyme deoxyhypusine hydroxylase. *Proc Natl Acad Sci USA* **111**, 8031–8036.
49 Sherman F (2002) Getting started with yeast. *Methods Enzymol* **350**, 3–41.
50 Molik S, Lill R and Muhlenhoff U (2007) Methods for studying iron metabolism in yeast mitochondria. *Methods Cell Biol* **80**, 261–280.
51 Stehling O, Smith PM, Biederbick A, Balk J, Lill R and Muhlenhoff U (2007) Investigation of iron-sulfur protein maturation in eukaryotes. *Methods Mol Biol* **372**, 325–342.
52 Pierik AJ, Netz DJ and Lill R (2009) Analysis of iron-sulfur protein maturation in eukaryotes. *Nat Protoc* **4**, 753–766.
53 Stehling O, Vashisht AA, Mascarenhas J, Jonsson ZO, Sharma T, Netz DJA, Pierik AJ, Wohlschlegel JA and Lill R (2012) MMS19 assembles iron-sulfur proteins required for DNA metabolism and genomic integrity. *Science* **337**, 195–199.
54 Harlow E and Lane D (1998) Using Antibodies: A Laboratory Manual. Cold Spring Harbor Laboratory, Cold Spring Harbor, NY.
55 Gupta M and Outten CE (2020) Iron-sulfur cluster signaling: the common thread in fungal iron regulation. *Curr Opin Chem Biol* **55**, 189–201.
56 Muhlenhoff U, Braymer JJ, Christ S, Rietzschel N, Uzarska MA, Weiler BD and Lill R (2020) Glutaredoxins and iron-sulfur protein biogenesis at the interface of redox biology and iron metabolism. *Biol Chem* **401**, 1407–1428.
57 Borkovich KA, Farrelly FW, Finkelstein DB, Taulien J and Lindquist S (1989) hsp82 is an essential protein that is required in higher concentrations for growth of cells at higher temperatures. *Mol Cell Biol* **9**, 3919–3930.
58 Netz DJ, Stumpfig M, Dore C, Muhlenhoff U, Pierik AJ and Lill R (2010) Tah18 transfers electrons to Dre2 in cytosolic iron-sulfur protein biogenesis. *Nat Chem Biol* **6**, 758–765.
59 Kimura Y, Yahara I and Lindquist S (1995) Role of the protein chaperone YDJ1 in establishing Hsp90-mediated signal transduction pathways. *Science* **268**, 1362–1365.
60 Voos W and Rottgers K (2002) Molecular chaperones as essential mediators of mitochondrial biogenesis. *Biochim Biophys Acta* **1592**, 51–62.
61 Westermann B, Gaume B, Herrmann JM, Neupert W and Schwarz E (1996) Role of the mitochondrial DnaJ homolog Mdj1p as a chaperone for mitochondrially synthesized and imported proteins. *Mol Cell Biol* **16**, 7063–7071.
62 Silberstein S, Schlenstedt G, Silver PA and Gilmore R (1998) A role for the DnaJ homologue Scj1p in protein

folding in the yeast endoplasmic reticulum. *J Cell Biol* **143**, 921–933.
63 Schwarz E, Westermann B, Caplan AJ, Ludwig G and Neupert W (1994) XDJ1, a gene encoding a novel non-essential DnaJ homologue from *Saccharomyces cerevisiae*. *Gene* **145**, 121–124.
64 Schwartz K, Wenger JW, Dunn B and Sherlock G (2012) APJ1 and GRE3 homologs work in concert to allow growth in xylose in a natural *Saccharomyces sensu* stricto hybrid yeast. *Genetics* **191**, 621–632.
65 Sluder IT, Nitika KLE and Truman AW (2018) The Hsp70 co-chaperone Ydj1/HDJ2 regulates ribonucleotide reductase activity. *PLoS Genet* **14**, e1007462.
66 Rowley N, Prip-Buus C, Westermann B, Brown C, Schwarz E, Barrell B and Neupert W (1994) Mdj1p, a novel chaperone of the DnaJ family, is involved in mitochondrial biogenesis and protein folding. *Cell* **77**, 249–259.
67 Li J, Qian X and Sha B (2003) The crystal structure of the yeast Hsp40 Ydj1 complexed with its peptide substrate. *Structure* **11**, 1475–1483.

Supporting information

Additional supporting information may be found online in the Supporting Information section at the end of the article.

Fig. S1. Components and pathways of cellular Fe/S protein biogenesis and iron regulation in fungi.
Fig. S2. No role of Pih1 in Fe/S protein maturation and iron regulation.
Fig. S3. Confirmation of the phenotype of GalL-HSC82/hsp82Δ cells.
Fig. S4. Protein sequence and structural analyses of DnaJ-related proteins containing Zn-finger-like regions.
Fig. S5. Confirmation of the phenotype of Gal-MDJ1 and *mdj1Δ* cells.
Fig. S6. No role of Mdj1 in cellular Fe/S protein maturation in *S. cerevisiae*.
Fig. S7. Ydj1 binds iron upon expression in *E. coli*.
Table S1. Yeast strains.
Table S2. Plasmids.